PROTEINS: Structure, Function, and Genetics 10:92–105 (1991)

The Crystal Structure of Staphylococcal Nuclease Refined at 1.7 Å Resolution

Thomas R. Hynes[1,3] and Robert O. Fox[1,2]

[1]Department of Molecular Biophysics and Biochemistry and the [2]Howard Hughes Medical Institute, Yale University, 260 Whitney Ave., New Haven, Connecticut 06511, and [3]Department of Cell Biology, Stanford University Medical School, Stanford, California 94305

ABSTRACT **The crystal structure of staphylococcal nuclease has been determined to 1.7 Å resolution with a final *R*-factor of 16.2% using stereochemically restrained Hendrickson–Konnert least-squares refinement. The structure reveals a number of conformational changes relative to the structure of the ternary complex of staphylococcal nuclease[1,2] bound with deoxythymidine-3′,5′-diphosphate and Ca^{2+}. Tyr-113 and Tyr-115, which pack against the nucleotide base in the nuclease complex, are rotated outward creating a more open binding pocket in the absence of nucleotide. The side chains of Ca^{2+} ligands Asp-21 and Asp-40 shift as does Glu-43, the proposed general base in the hydrolysis of the 5′-phosphodiester bond. The significance of some changes in the catalytic site is uncertain due to the intrusion of a symmetry related Lys-70 side chain which hydrogen bonds to both Asp-21 and Glu-43. The position of a flexible loop centered around residue 50 is altered, most likely due to conformational changes propagated from the Ca^{2+} site. The side chains of Arg-35, Lys-84, Tyr-85, and Arg-87, which hydrogen bond to the 3′- and 5′-phosphates of the nucleotide in the nuclease complex, are unchanged in conformation, with packing interactions with adjacent protein side chains sufficient to fix the geometry in the absence of ligand. The nuclease structure presented here, in combination with the stereochemically restrained refinement of the nuclease complex structure[2] at 1.65 Å, provides a wealth of structural information for the increasing number of studies using staphylococcal nuclease as a model system of protein structure and function.**

Key words: protein structure, ligand binding, crystallographic refinement, phosphodiesterase, calcium ligands

INTRODUCTION

Staphylococcal nuclease (nuclease) is a small globular protein of 149 residues containing no disulfide links, which reversibly folds to yield the active enzyme. Nuclease catalyzes the hydrolysis of the phosphate backbone of DNA and RNA leaving 3′-phosphate mononucleotides and dinucleotides.[3] Nuclease has been extensively used as a model protein for the study of enzymatic mechanism, thermodynamic stability, and the kinetics of refolding.[1,4–10] Renewed interest in nuclease has come from the application of site-directed mutagenesis as a probe of protein stability,[11] folding, enzymatic mechanism,[12,13] as well as structural studies employing X-ray diffraction[14,15] and NMR methods.[16–18]

In this paper we present the structure of nuclease refined to 1.7 Å resolution with a final *R*-factor of 16.2% using stereochemically restrained Hendrickson–Konnert least-squares refinement.[19] The RMS deviations in bond distance and bond angle distance are 0.015 and 0.033 Å, respectively. The estimated mean error in atomic position is 0.18 Å (Fig. 1). An unrefined structure of nuclease at 2.0 Å resolution has been described[20] although the coordinates are not available in the Brookhaven Protein Data Base.[21] The crystal structure of the ternary complex of nuclease (nuclease complex) bound with deoxythymidine-3′,5′-diphosphate (pdTp) and Ca^{2+} was originally determined at 1.5 Å resolution[1,22] (2SNS, Brookhaven Protein Data Base). Loll and Lattman have recollected diffraction data on the nuclease complex and refined the structure to 1.65 Å resolution using Hendrickson–Konnert least-squares refinement.[2]

MATERIALS AND METHODS

Crystallization

Nuclease was expressed in *Escherichia coli* strain AR120 containing a pAS1 vector carrying the nuclease gene cloned from *Staphylococcus aureus* Foggi strain, under the control of the lambda pL promoter (Goodman and Fox, in preparation). Protein was purified to >95% purity on a phosphocel-

Received August 9, 1990; accepted September 25, 1990.

Address reprint requests to Dr. Robert O. Fox, Department of Molecular Biophysics and Biochemistry and the Howard Hughes Medical Institution, Yale University, 260 Whitney Avenue, New Haven, CT 06511.

Present address of T.R. Hynes: Genentech, Inc., 460 Point San Bruno Blvd., South San Francisco, CA 94080.

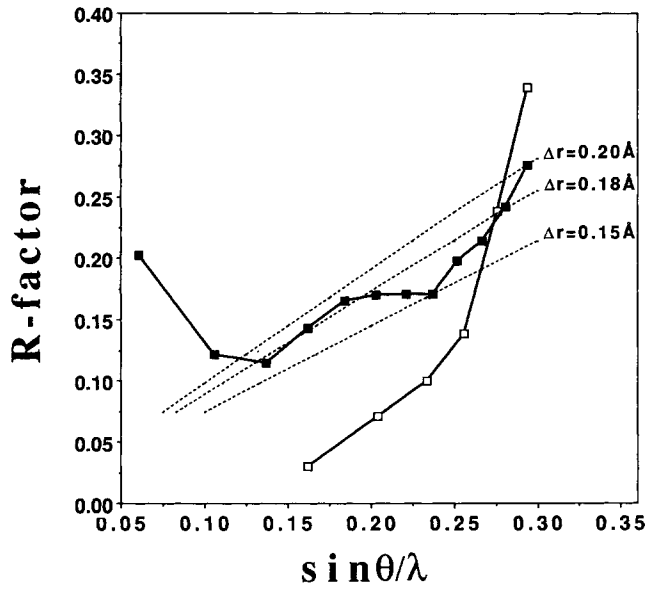

Fig. 1. Luzzati plot estimate of the mean error in atomic position. Filled squares, crystallographic *R*-factor ($R = \Sigma | F_o - F_c | / \Sigma | F_o |$) as a function of resolution from the final refinement cycle. The dotted lines are theoretical curves assuming three values of mean absolute error in atomic position (Δr).[29] Open squares, symmetry *R*-factor of measured intensities as a function of resolution for data processed with XENGEN version 1.3.

lulose column eluted with a linear gradient from 0.3 M ammonium acetate pH 6.0 to 1.0 M ammonium acetate pH 8.0. The protein solution was passed over a DEAE column to remove contaminating DNA followed by dialysis against 0.2 M NaCl and distilled water as described.[16] The purified protein was stored lyophilized at −20°C.

Nuclease crystals were grown out of low salt buffer using 2-methyl-2,4-pentanediol (MPD) (Aldrich, Gold Label) as a precipitant.[23] Lyophilized nuclease was dissolved in crystallization buffer (10.5 mM potassium phosphate, pH 8.15 at 25°C) to a final concentration of 2 mg/ml. MPD was added dropwise with mixing to a final concentration of 22% (w/w). The solution was allowed to stand at least 24 hr at 5°C and then filtered through a 0.45 μm Millipore filter to remove any precipitate. MPD was then added to final concentrations over a range of 26–30% (w/w) and 0.75 ml aliquots of the solution transferred to siliconized 6×50 mm glass test tubes, sealed with parafilm, and stored at 5°C. Bipyramidal crystals suitable for data collection (~0.4 × 0.4 × 0.6 mm) generally grew within 1 month. The space group of the nuclease crystals is $P4_1$ with unit cell dimensions within 1% of values of the nuclease complex.[2]

X-Ray Data Collection

Diffraction data from a single nuclease crystal ($a = b = 48.5$ Å, $c = 63.5$ Å) was collected to 1.7 Å resolution at 25°C using the Nicolet-Xentronics area detector system at Yale University. CuK_α X-rays (1.54 Å) were generated with an Elliot GX-6 rotating anode running at 50 kV/50 mA and equipped with a graphite monochrometer. Each data frame covered a 0.2° oscillation range with counts accumulated for 120 sec/frame; 38,517 measurements of 14,893 unique reflections were collected, covering 93% of the possible reflections to 1.7 Å. Reflection data were processed with XENGEN version 1.1 software[24] and used in the initial stages of refinement. Reflection data were reprocessed from the raw data frames when XENGEN version 1.3 became available and utilized in the final rounds of refinement as described below. The merging *R*-factor on intensity for symmetry related reflections was 5.1% (Fig. 1). The D2 value suggested by Howard (A. J. Howard, personal communication), corresponding to the highest resolution shell of data with an average intensity greater than 2σ, was 1.85 Å.

Refinement

The starting model and phases for the refinement of nuclease were taken from the structure of an unliganded point mutant of nuclease refined in this laboratory (P117G) which in turn was based on the 1.5 Å structure of the nuclease complex in the Brookhaven Protein Data Base (2SNS).[1] The starting model consisted of the protein atoms of the P117G structure including refined individual temperature factors.

Nuclease crystals display anisotropic diffraction with stronger amplitudes along the c^* axis relative to the a^* and b^* axes. A local scale factor[25] was calculated and applied to the observed structure factor amplitudes (F_{obs}) relative to the calculated struc-

Table I. Crystallographic Parameters at the End of Refinement

R-factor*	16.2 %
Resolution range	8–1.7 Å
$<F_o-F_c>$	21.9
σ weight†	16.0
σ cutoff	2.0
Number of reflections	12359
Number of protein atoms	1091
Number of water molecules	85
Mean B§	22.46 Å^2
R.m.s. coordinate shift of final cycle	0.01 Å

*R-factor = $\Sigma \mid F_o-F_c \mid / \Sigma \mid F_o \mid$.
†Weight applied to structure factors in refinement was $1/\sigma^2$.
§$B = 8\pi^2(\overline{u^2})$ = mean square amplitude of atomic vibration.

Table II. Final Weighting Parameters and Deviations From Ideal Geometry*

Restraint	R.m.s. deviation	Target σ†
Distances (Å)		
Bond distance	0.015	0.020
Angle distance	0.033	0.030
Planar 1–4 distance	0.037	0.030
Planar groups (Å)	0.014	0.020
Chiral volumes (Å^3)	0.178	0.150
Non-bonded contacts (Å)		
Single torsion contacts	0.162	0.200
Multiple torsion contacts	0.153	0.200
Possible hydrogen bonds	0.157	0.200
Torsional angles (degrees)		
Planar	2.8	3.0
Staggered	16.6	15.0
Orthonormal	18.7	20.0
Thermal factors (Å^2)		
Main chain bond	1.0	1.2
Main chain angle	1.7	1.8
Side chain bond	5.5	4.0
Side chain angle	8.4	6.0

*See Hendrickson, 1985.
†Weight applied to geometry restraints in refinement was 1/(target σ)^2.

ture factor amplitudes (F_{calc}). The scale factor was calculated as $\Sigma(F_{calc})/\Sigma(F_{obs})$ and excluded the central reflection to prevent bias. The box size for the local scale was $5\times5\times5$, with any reflection having fewer than 40 observed reflections in the box eliminated from the data set. The local scale was applied once in the early stages of refinement and then recalculated and applied to the original unscaled data set at the end of the refinement.

The initial stages of the nuclease refinement used the program XPLOR,[26] which employs molecular dynamics restrained by the crystallographic data to increase the radius of convergence of the crystallographic refinement. The method has been shown to reduce the number of manual model building sessions needed to reach the final structure.[27] In the final stages of the refinement we switched to Hendrickson–Konnert least-squares refinement[19] so that the geometric restraints matched those used in the refinement of the nuclease complex structure[2] to facilitate direct comparison of the two structures.

All stages of energy minimization and molecular dynamics using XPLOR were performed over the resolution range of 8–2.0 Å with the difference between the observed and calculated structure factor amplitudes included as a weighted term in the total energy equation. The weight (W_a) used in all stages of XPLOR refinement was 77894 kcal mol^{-1}. The weight was calculated so that the gradient of the diffraction data (E_x) equals the gradient of the empirical potential energy (E_i).[27] The initial R-factor between observed nuclease structure factor amplitudes, local scaled as described above, and the starting model was 30.1%. Using XPLOR the model first underwent 40 cycles of energy minimization dropping the R-factor to 25.1% while at the same time relieving bad contacts prior to the molecular dynamics refinement. The model was then subjected to 0.5 psec of molecular dynamics at 1000 K followed by 0.25 psec at 300 K. The time step of integration was 1.0 fsec. Following 40 cycles of energy minimization the R-factor was 23.5%. Refinement of the individual temperature factors dropped the R-factor to 22.1%. The model then underwent 1.0 psec of molecular dynamics at 1500 K followed by 0.25 psec at 300 K. Following 40 cycles of energy minimization the R-factor had dropped to 21.3%. The entire refinement with XPLOR required 9 hr of cpu time on a VAX 8800. This stage was reached without manual model building and did not include solvent molecules.

Examination of $2F_o-F_c$ and F_o-F_c electron density maps at this stage demonstrated an excellent fit of the model to the density over the length of the protein chain with the exception of the region of the point mutation at residue 117 in the starting model. This region adopts a very different conformation in the P117G mutant including a 180° difference in the isomerization state of the peptide bond preceding residue 117. The correct conformation for this region was clearly indicated in the F_o-F_c map and easily built into electron density using FRODO.[28] Sixty-eight water molecules were also placed into positive electron density in the F_o-F_c difference map. All water molecules included were within hydrogen bonding distance to protein hydrogen bond donor or acceptor atoms.

This model was then subjected to cycles of Hendrickson–Konnert refinement with the high resolution range extended from 2.0 to 1.8 Å, converging to an R-factor of 18.5%. The model was then reexamined, additional waters added, and minor corrections made to the protein model as indicated by $2F_o-F_c$ and F_o-F_c electron density maps. At this point re-

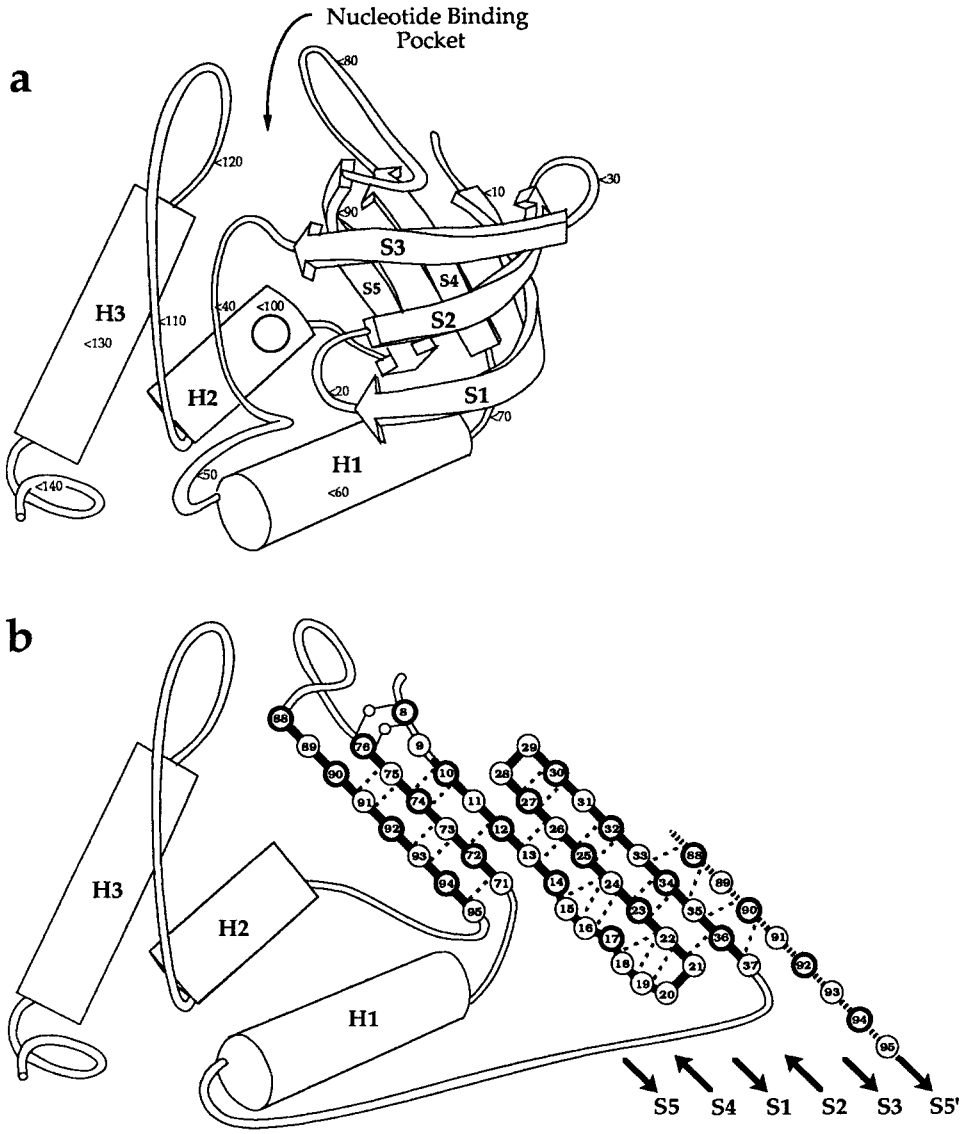

Fig. 2. Tertiary fold and hydrogen bonding of nuclease. **(a)** Overall fold of nuclease represented by cylinders (α-helices) and arrows (β-sheets). The five β-strands, labeled S1–S5, form a five-stranded β-barrel. The three α-helices are labeled H1–H3. The nucleotide binding pocket is indicated by the arrow and the Ca^{2+} binding site by the large circle. The figure was drawn with the aid of ARPLOT.[35] **(b)** The β-barrel of nuclease unrolled to illustrate the hydrogen bonding pattern between the β-strands. Hydrogen bonds are indicated by the dashed lines. Numbered residues with dark circles project side chains into the hydrophobic core of the β-barrel, residues with light circles project outward. S5′ is a duplication of S5 showing the parallel hydrogen bonding pattern between S5 and S3. Two water molecules form bridging hydrogen bonds between residues 8 and 76 as indicated by the small circles and solid lines. Two classic β-bulges[30] with branched hydrogen bonds are found between S1 and S2 (residues 15, 16, 24 and 18, 19, 22). β-strand hydrogen bond distances listed in Table VI are ordered top to bottom, left to right as shown in the figure.

flection data reprocessed with XENGEN version 1.3 were introduced. Only structure factor amplitudes greater than 2σ were used in the final cycles of refinement. Waters were refined with individual temperature factors with occupancies set to 1.0. Water molecules which refined to a temperature factor greater than 60 $Å^2$ were eliminated from the model. The resolution range was extended to cover 8–1.7 Å and refined to convergence. The final R-factor is 16.2% for amplitudes greater than 2σ. The overall temperature factor is 22.5 $Å^2$. Tables I and II summarize the final refinement parameters and geometry of the structure. From a Luzzati plot[29] (Fig. 1) the mean absolute error in atomic position is estimated to be 0.18 Å.

RESULTS AND DISCUSSION

Polypeptide Conformation

The overall tertiary fold of nuclease is composed of a highly twisted five stranded β-barrel and three α-helices (Fig. 2). The residue ranges of secondary structure elements are listed in Table III. Details of

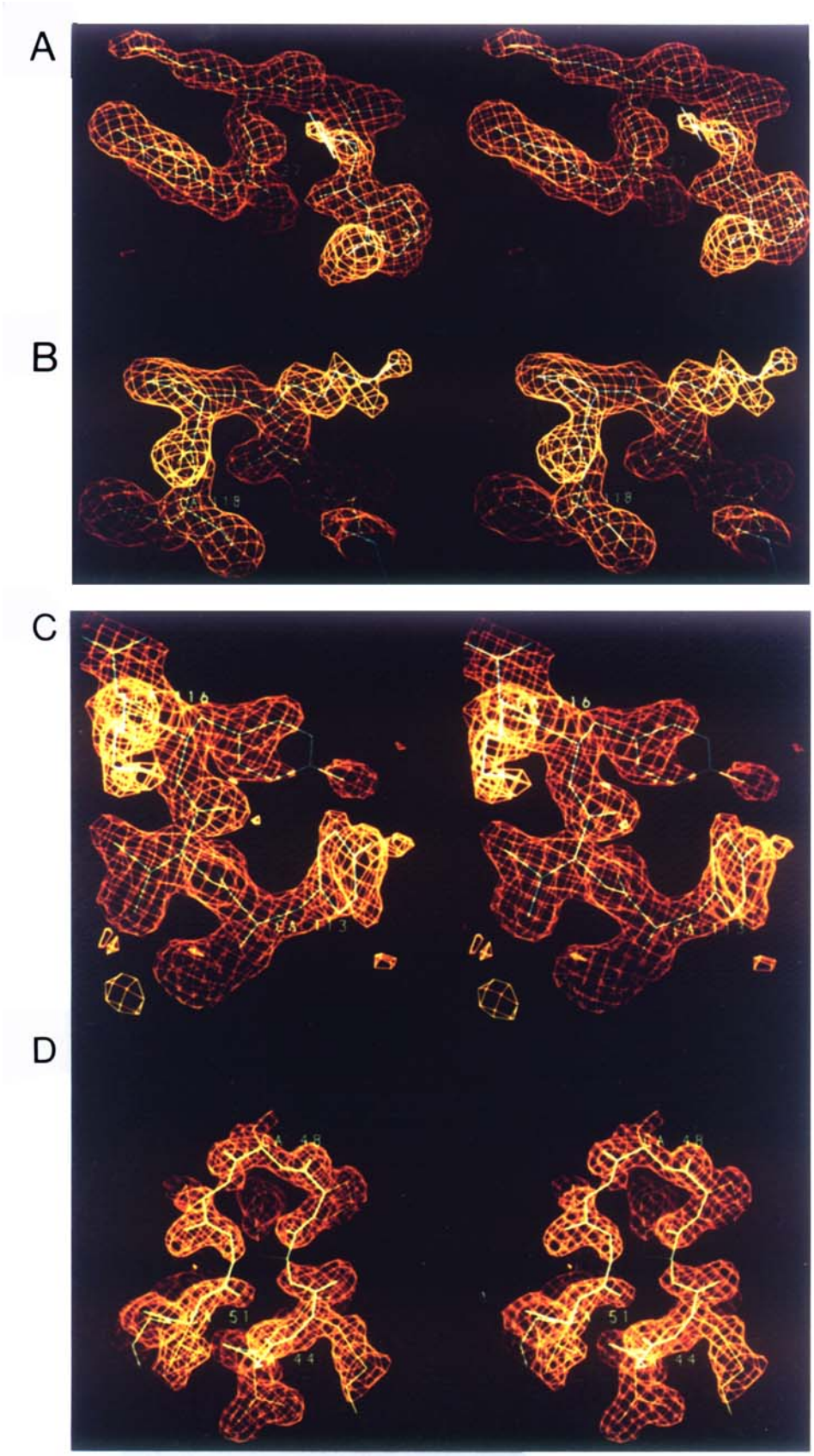

Fig. 3. Residue delete electron density maps of nuclease. All *maps are 1.7 Å F_o-F_c residue delete electron density maps contoured at 2.5σ (σ is the root-mean-square difference electron density in the unit cell).* The indicated residues were omitted from the F_o-F_c Fourier map calculations in order to remove the bias of phase information contributed by the model. **(a)** Structure of the type I′ β-turn (residues 27–30). Residues 27–31 (Tyr-Lys-Gly-Gln-Pro) were omitted from the map calculation. **(b)** Structure of the type VI_a β-turn in nuclease (residues 115–118; Tyr-Lys-Pro-Asn) *including a cis peptide bond for Pro-117. Residues 113–118 were omitted from the map calculation.* **(c)** *Structure of nuclease* residues 113–116 (Tyr-Val-Tyr-Lys). Residues 113–118 were omitted from the map calculation. **(d)** Structure of the flexible loop of nuclease (residues 43–52). Residues 43–52 (Glu-Thr-Lys-His-Pro-Lys-Lys-Gly-Val-Glu) were omitted from the F_o-F_c Fourier map calculation.

Table III. Secondary Structure

α-Helix			Residue range
1			54–68
2			98–106
3			121–135
β-strand*			**Residue range**
1			10–19
2			22–27
3			30–36
4			71–76
5			88–95
β-bulge			**Residues**
1			15,16,24
2			18,19,22
β-turn	**turn type**	**O_i-N_{i+3} (Å)**	**Residue range**
1	I	3.31	19–22
2	I′	3.22	27–30
3	I	3.81	46–49
4	II	3.00	52–55
5	I	2.97	83–86
6	I′	2.84	94–97
7	VI_a	2.96	115–118
8	I	3.11	119–122
9	II′	2.82	137–140
10	I	2.95	138–141
		Ave = 3.10	

*The residue ranges of β-strands are determined by hydrogen bonding to adjacent β-strands (Fig. 11b) as well as backbone geometry.

TABLE IV. Side Chains Atoms Lacking Density

	No $2F_o-F_c$ density beyond	
Lys	6	CB
Gln	30	CB
Lys	48	CG
Lys	64	CB
Lys	78	CE
Lys	97	CG
Lys	133	CE
Lys	134	CD

backbone and side chain conformation are well delineated in electron density maps (Fig. 3). Residues listed in Table IV, primarily lysines, lack side chain density to the indicated extent.

Electron density is not observed for the first five residues of nuclease which are presumed to be disordered. Residues 6–9 adopt β-strand geometry and are held by a pair of well ordered water molecules that bridge between His-8 and Phe-76 on β-strand 4 (Fig. 2b, Fig. 4b). Residues 10–19 adopt an extended β-strand conformation (β-strand 1), integral to the five stranded β-barrel of nuclease. A five-stranded β-barrel represents the smallest observed size in terms of strand number, and requires highly twisted β-strands to close the β-barrel[30] (Fig. 2a). The twist of β-strands 1 and 2 is augmented by two classic β-bulges[30] adjacent to the first β-turn (Fig. 2b, Table III).

β-Strand 2 leads back to the top of the β-barrel to a type I′ β-turn (residues 27–30) clearly outlined in electron density (Fig. 3a). The type I′ β-turn conformation differs from the distorted loop in the earlier nuclease complex structure (2SNS)[1] but agrees closely with the recently refined structure.[2] The type I′ β-turn conformation is commonly found joining antiparallel β-strands.[31] The conformation of this β-turn is of interest as the sequence of this β-turn has been subjected to extensive random mutagenesis to determine the range of amino acid sequences which permit the protein to fold (Goodman and Fox, in preparation). In addition the β-turn location has been used as a host site for the introduction of a five residue turn structure from concanavalin A.[14]

Following β-strand 3 which descends the front of the β-barrel, the chain crosses the floor of the binding pocket and enters a large flexible loop centered around residue 50. The electron density from residue 45 to 52 is weak but clear (Fig. 3d), mirrored by the elevated temperature factors over this region (Fig. 5). The loop in nuclease is shifted relative to the nuclease complex and differs in the details of backbone and side chain geometry (see below). Helix 1 follows, extending across the bottom of the β-barrel. The hydrogen bonding at the N-terminal end of the helix is punctuated by Pro-56. A salt bridge internal to the helix links the side chains of Lys-63 and Glu-67. This configuration has been shown to increase the stability of helical peptides in solution[32] and may play a stabilizing role in nuclease.

β-Strand 4 extends up the back of the β-barrel into a loop centered around residue 80. The loop contributes residues to the right half of the nucleotide binding pocket including Lys-84, Tyr-85, and Arg-87 which hydrogen bond to the 3′- and 5′-phosphates in the nuclease complex. β-Strand 5 extends down the back of the β-barrel forming parallel β-sheet interactions with β-strand 3 and antiparallel β-sheet interactions with β-strand 4 (Fig. 2b). Helix 2 crosses the back of the molecule and is terminated by a single turn of 3_{10} helix. The chain adopts an extended conformation up and along the left side of the binding pocket to β-turn 7, a type VI_a β-turn, including a *cis*-Pro (residues 115–118, see below). The final length of the nuclease chain leads into helix 3, terminated by one turn of 3_{10} helix. The constrained torsion angles of a type II′ β-turn conformation (residues 137–140) places Asn-138 outside the sterically favorable regions of ϕ,ψ space (Fig. 6). A single water molecule is buried near the C-terminus, hydrogen bonded to the indol nitrogen of Trp-140 and the backbone carbonyl oxygens of Val-104 and Ala-109.

Table V. α-Helix Hydrogen Bonds

Helix	Donor (D)			Acceptor (A)			D-A distance (Å)	D-H-A angle* (deg)
1	A	58	N	Y	54	O	2.93	22.8
	S	59	N	G	55	O	2.91	24.5
	A	60	N	P	56	O	2.91	26.8
	F	61	N	E	57	O	2.98	23.5
	T	62	N	A	58	O	3.14	2.8
	K	63	N	S	59	O	3.23	16.0
	K	64	N	A	60	O	2.98	14.7
	M	65	N	F	61	O	3.00	21.5
	V	66	N	T	62	O	2.98	24.7
	E	67	N	K	63	O	2.81	31.9
	N	68	N	K	64	O	3.07	32.8
2	A	102	N	M	98	O	3.04	13.9
	L	103	N	V	99	O	3.03	15.0
	V	104	N	N	100	O	3.44	19.1
	R	105	N	E	101	O	2.75	13.4
	Q	106	N	A	102	O	3.14	34.9
3	L	125	N	H	121	O	2.90	17.4
	R	126	N	E	122	O	2.84	25.6
	K	127	N	Q	123	O	2.95	26.7
	S	128	N	H	124	O	3.17	22.3
	E	129	N	L	125	O	2.90	28.0
	A	130	N	R	126	O	3.05	27.4
	Q	131	N	K	127	O	3.13	20.6
	A	132	N	S	128	O	3.01	22.4
	K	133	N	E	129	O	2.84	29.8
	K	134	N	A	130	O	2.97	19.2
	E	135	N	Q	131	O	2.98	38.1
	K	136	N	A	132	O	3.01	72.3
							Ave = 2.85	

*Angular deviation from a linear bond. Hydrogen positions were calculated using the program XPLOR.[26]

As was the case in the nuclease complex, protein density is not observed beyond Ser-141.

Comparison of Nuclease and the Nuclease Complex

Focusing on changes between the structure of nuclease and the nuclease complex, the major elements of secondary structure, namely the five-stranded β-barrel and the three α-helices are unchanged with a RMS deviation of 0.24 Å between backbone atoms (Fig. 7a). This demonstrates that large-scale motions of domains or secondary structure elements does not occur upon substrate binding. This is perhaps not surprising given the small compact shape of nuclease. Changes in backbone conformation are limited to the flexible loop centered around residue 50 and the short segment including Tyr-113 and Tyr-115. The remaining differences are in side chain orientation, and occur primarily in the Ca^{2+} binding site region.

Nucleotide Binding Site

A prominent feature in the nuclease complex are two tyrosines (Tyr-113 and Tyr-115) which form the left side of the nucleotide binding pocket. In the absence of nucleotide the binding pocket adopts a more open conformation (Fig. 7a,b), where the side chain of Tyr-113 is further removed from the binding pocket and packs against Tyr-115. Tyr-115 rotates outward to a smaller extent. The electron density for the tyrosine side chains is weak but unambiguous in an F_o-F_c residue delete electron density map (Fig. 3c). The side chains of Tyr-113 and Tyr-115 are highly exposed to solvent and have average temperature factors of 39.8 and 47.0 $Å^2$, respectively. The backbone conformation of residues 113–115 is well determined with an average temperature factor of 24.5 $Å^2$. In the absence of nucleotide the backbone ϕ,ψ angles of residues 112–115 correspond to that of an extended β-sheet. With bound nucleotide Tyr-113 adopts a left-handed helix conformation. Therefore the transformation between the open pocket of nuclease and the closed state of the nuclease complex involves switching between discrete energy minima of backbone conformation.

Following the two Tyr residues is a type VI_a β-turn[30] (residues 115–118; Tyr-Lys-Pro-Asn) including a *cis*-Pro at residue 117 (Fig. 3b). The conformation of this β-turn in nuclease is of great interest as NMR studies have demonstrated that in the absence of nucleotide a minor folded form occurs differing in the *cis/trans* isomerization state of Pro 117.[33,34] The

Table VI. β-Sheet Hydrogen Bonds

β-strand* pair	Donor (D)			Acceptor (A)			D-A distance (Å)	D-H-A angle (deg)
5:4	Y	91	N	E	75	O	2.92	7.6
	E	75	N	Y	91	O	2.95	33.0
	Y	93	N	E	73	O	2.83	12.6
	E	73	N	Y	93	O	2.93	18.4
	D	95	N	K	71	O	2.96	7.3
4:1	E	10	N	V	74	O	2.90	16.5
	V	74	N	E	10	O	2.79	17.2
	A	12	N	I	72	O	3.12	32.5
1:2	T	13	N	M	26	O	3.07	20.9
	M	26	N	T	13	O	2.70	9.3
	I	15	N	K	24	O	3.00	29.7
	K	16	N	K	24	O	3.06	12.0
	K	24	N	K	16	O	2.73	14.7
	I	18	N	T	22	O	3.09	28.2
	D	19	N	T	22	O	3.09	17.0
	T	22	N	D	19	O	3.31	20.1
2:3	Q	30	N	Y	27	O	3.22	22.3
	Y	27	N	Q	30	O	2.79	3.6
	M	32	N	L	25	O	2.76	28.3
	L	25	N	M	32	O	2.76	19.2
	F	34	N	V	23	O	2.64	10.9
	V	23	N	F	34	O	2.99	21.8
	L	36	N	D	21	O	2.96	10.1
3:5	G	88	N	T	33	O	2.90	21.1
	R	35	N	G	88	O	2.80	11.2
	A	90	N	R	35	O	3.47	17.0
	L	37	N	A	90	O	2.98	4.2
							Ave = 2.95	

*β-strand hydrogen bond distances are ordered as shown in Fig. 11b going top to bottom, left to right.

Table VII. Main Chain to Main Chain Hydrogen Bonds

Donor (D)			Acceptor (A)			D-A distance (Å)	D-H-A angle (deg)
D	40	N	K	110	O	2.88	13.0
H	46	N	G	50	O	2.69	24.3
G	50	N	H	46	O	2.76	41.1
E	52	N	E	43	O	2.89	1.6
G	55	N	E	52	O	3.00	33.7
D	83	N	R	87	O	2.85	27.6
G	86	N	D	83	O	2.97	20.4
L	89	N	R	81	O	2.80	26.1
A	94	N	K	97	O	2.88	10.5
K	97	N	A	94	O	2.84	16.8
V	99	N	I	92	O	2.77	16.5
G	107	N	V	104	O	3.12	17.1
L	108	N	L	103	O	2.92	22.4
K	110	N	D	40	O	2.96	15.9
A	112	N	L	38	O	2.87	7.1
N	118	N	Y	115	O	2.96	42.6
N	119	N	P	117	O	2.97	39.2
E	122	N	N	119	O	3.11	20.2
K	136	N	K	133	O	2.92	31.7
L	137	N	A	132	O	3.27	7.0
I	139	N	G	107	O	2.99	18.9
W	140	N	L	137	O	2.82	22.0
S	141	N	N	138	O	2.95	14.4
						Ave = 2.92	

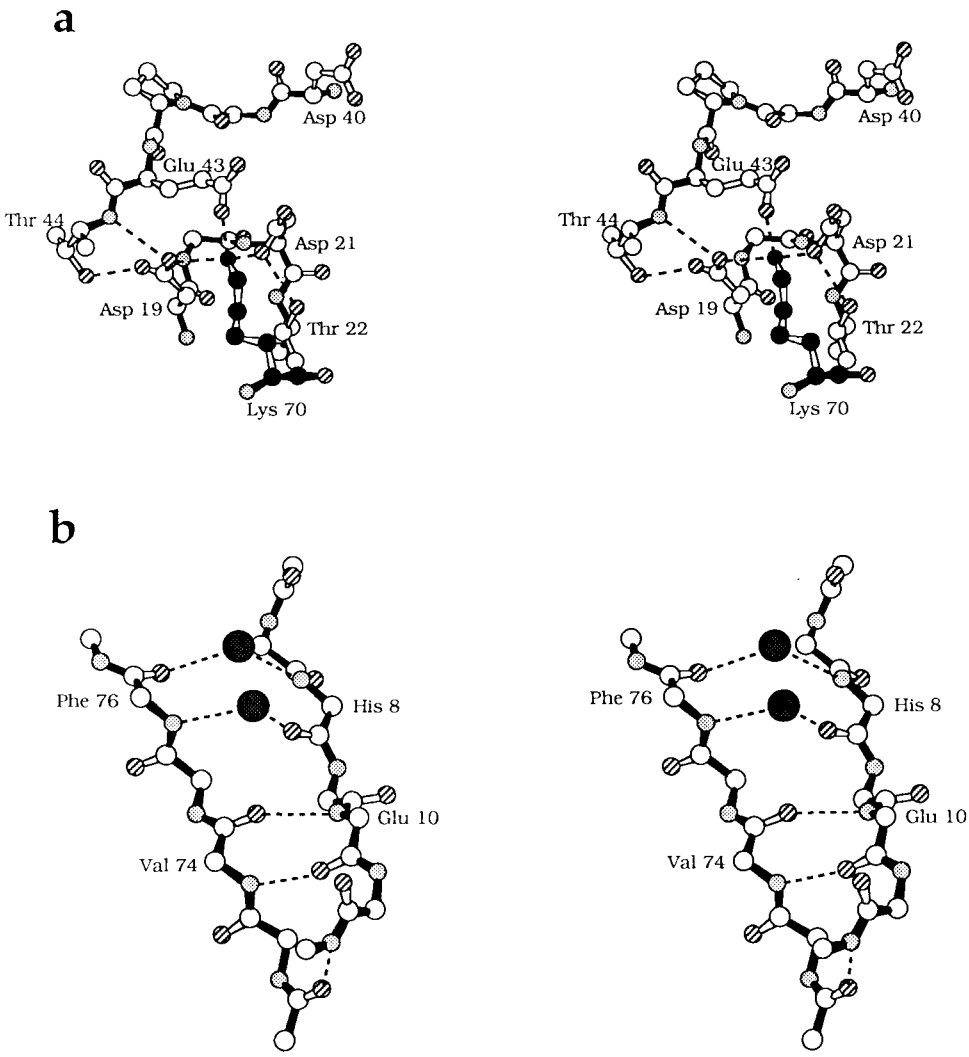

Fig. 4. Symmetry-related and water-bridged hydrogen bonds. Oxygen atoms are shown with diagonal lines, nitrogen atoms are shaded, and hydrogen bonds are shown by dashed lines. **(a)** Lys-70 from a symmetry-related molecule, shown with filled atoms, hydrogen bonding to the side chains of Asp-19, Asp-21, and Glu-43. **(b)** Water-bridged hydrogen bonds connecting backbone atoms of residues 8 and 76. The pair of hydrogen bonds between residues 10 and 74 is also included for comparison. Waters are represented by the large spheres. Side chain atoms are omitted for clarity.

minor folded form is titrated away with the addition of pdTp and Ca^{2+}.[16] Approximately 10% of the molecules adopt the minor folded conformation (25°C, pH 5.5), which was shown to be in free exchange with the major species.[34] Density indicative of heterogeneity in the isomerization state of the peptide bond in nuclease is not observed (Fig. 3b). As it would be difficult to observe a 10% *trans* population, the observed density does not exclude the possibility of isomerization in the crystal environment. The presence of the *cis*-Pro conformation in nuclease and the nuclease complex indicates that the major folded form corresponds to the *cis*-isomer. The influence of the nucleotide inhibitor on the *cis/trans* equilibrium of Pro-117 presumably results from the mechanical linkage to Tyr-113 and Tyr-115.

Ca^{2+} Binding Site

In the nuclease complex structure a single Ca^{2+} is liganded to the protein through the side chain carboxylates of Asp-21, Asp-40, and the backbone carbonyl oxygen of Thr-41. The side chain of Glu-43 is bridged by water molecules to both the Ca^{2+} and the 5′-phosphate of the nucleotide and is thought to play the role of a general base in the cleavage of the 5′-phosphate.[1,2] In nuclease the side chains of Asp-40 and Glu-43 have rotated around x_1 by 120° relative to the nuclease complex (Fig. 7c). Asp-21 has moved in toward the Ca^{2+} site. A water molecule close to the Ca^{2+} position maintains hydrogen bonds with the side chain of Asp-21 and the backbone oxygen of Thr-41 but also hydrogen bonds to the backbone ni-

Table VIII. Main Chain to Side Chain Hydrogen Bonds

Donor (D)			Acceptor (A)			D-A distance (Å)	D-H-A angle (deg)
E	43	N	E	52	OE1	2.58	13.2
K	48	N	H	46	ND1	2.95	28.9
K	49	N	H	46	ND1	2.72	13.7
K	70	N	D	95	OD1	3.14	19.2
K	70	N	D	95	OD2	2.99	43.3
K	71	N	D	95	OD2	2.94	30.1
K	78	N	D	77	OD2	2.55	39.8
G	79	N	N	118	OD1	2.68	40.5
Y	85	N	D	83	OD1	2.79	40.2
G	86	N	D	83	OD1	3.06	74.8
R	87	N	D	83	OD1	2.92	24.7
I	92	N	N	100	OD1	2.99	15.1
V	111	N	E	129	OE1	2.80	10.4
T	120	N	D	77	OD1	2.89	29.8
H	121	N	Y	91	OH	3.38	7.5
T	62	OG1	G	20	O	2.75	—
R	35	NH1	L	36	O	2.72	68.8
N	100	ND2	L	37	O	2.82	24.1
R	35	NH1	V	39	O	2.78	19.7
R	35	NH2	V	39	O	3.17	43.3
N	118	ND2	Q	80	O	2.95	16.0
N	138	ND2	Q	106	O	2.64	9.7
S	141	OG	N	138	O	2.84	—
						Ave = 2.87	

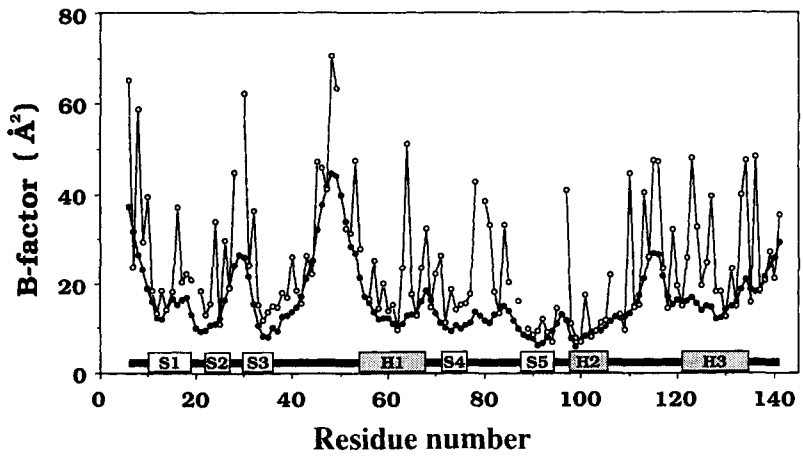

Fig. 5. Temperature factors of nuclease residues. Plot of main chain (filled circles) and side chain (open circles) temperature factors (*B*-factors). Breaks in the line connecting side chain temperature factors correspond to glycine residues. Elements of secondary structure as listed in Table III are indicated by the bars below.

trogen of Thr-41. Clouding the interpretation of changes in the Ca^{2+} site is the intrusion of the ϵ-amino of Lys-70 from a symmetry-related molecule in the crystal which forms hydrogen bonds to the side chains of Asp-19, Asp-21, and Glu-43 (Fig. 4a). It is therefore not possible in this case to attribute the observed changes in conformation solely to the absence of Ca^{2+}. A symmetry-related Lys-70 also extends into the Ca^{2+} site of the nuclease complex.[2] Binding studies in solution indicate that two Ca^{2+} ions bind to nuclease along with the pdTp inhibitor[3,5,6] although only one site is observed in the crystal. The second site may be filled by the Lys-70 side chain of the symmetry related molecule, composed of residues Asp-19, Asp-21, and Glu-43.

The large loop centered around residue 50 (residues 43–53) is highly exposed to solvent and has weak electron density indicative of a highly mobile region (Fig. 3d). The backbone conformation is clear and has shifted relative to the conformation of the same loop in the nuclease complex (Fig. 7a,c). A possible link between the loop and the bound pdTp and Ca^{2+} is the side chain of Glu-43 at the N-terminal end of the loop which is bridged by water molecules to both the Ca^{2+} and the 5′-phosphate of the nucle-

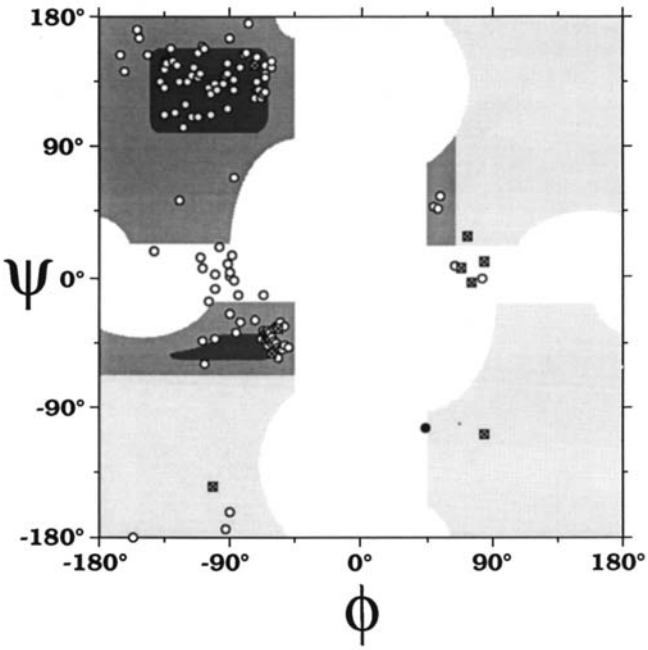

Fig. 6. Ramachandran plot of nuclease ϕ,ψ angles. All shaded areas represent the sterically allowed range of Gly. Non-Gly residues are restricted to the medium and dark shaded areas.[30] Gly residues are indicated by a cross inside a square. Asn-138 which lies significantly outside the allowed range is indicated by the filled circle (see text).

Table IX. Side Chain to Side Chain Hydrogen Bonds

Donor (D)			Acceptor (A)			D-A distance (Å)	D-H-A angle (deg)
T	22	OG1	D	21	OD2	2.91	—
Y	27	OH	E	10	OE2	2.72	—
R	35	NH2	D	40	OD1	3.14	46.9
T	44	OG1	D	19	OD2	2.87	—
Y	54	OH	S	141	OG	3.41	—
K	63	NZ	E	67	OE1	3.11	—
K	63	NZ	E	67	OE2	3.02	—
Y	85	OH	K	84	NZ	2.88	—
R	87	NE	D	83	OD2	2.83	44.8
R	87	NH1	D	83	OD2	3.06	45.8
Y	91	OH	D	77	OD1	2.64	—
Y	93	OH	E	75	OE2	2.59	—
R	105	NH1	E	135	OE1	2.78	47.3
R	105	NH2	E	135	OE2	2.98	22.2
T	120	OG1	D	77	OD2	2.63	—
H	121	NE2	E	75	OE2	3.06	25.4
R	126	NE	E	122	OE1	2.86	17.9
R	126	NH2	E	122	OE1	3.14	39.6
S	128	OG	E	101	OE2	2.61	—
Q	131	NE2	E	135	OE1	2.97	24.1
						Ave = 2.91	

otide in the nuclease complex. The divergence between the backbone atoms of nuclease and nuclease complex begins at Glu-43 and it is possible that the loss of interaction between the Glu-43 side chain and active site ligands leads to the altered loop conformation. An additional influence could be the side chain of Asp-19 which has rotated 180° around x_1 in nuclease and hydrogen bonds to the side chain of Thr-44 which is shifted with the loop toward Asp-19. Although Asp-19 faces the Ca^{2+} in the nuclease complex, it is not a direct ligand and therefore it is not possible to establish if the rotation of Asp-19 is a cause or an effect of the altered loop conformation (Fig. 4a, Fig. 7c).

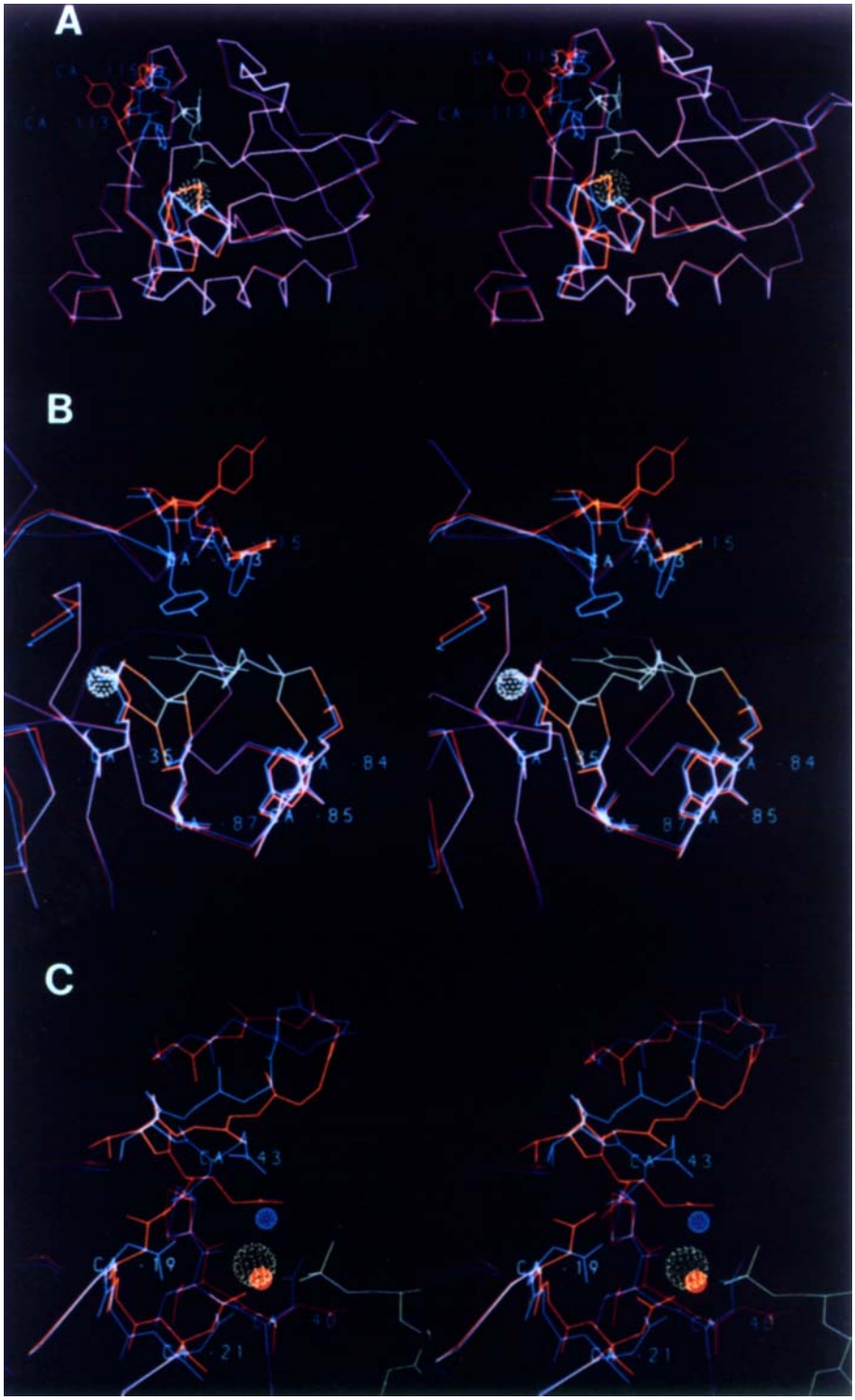

Fig. 7. Comparison of the structures of nuclease and the nuclease complex. **(a)** The complete backbone tracing of the nuclease structure (red) superimposed on the backbone of the nuclease complex structure[2] (blue). α-Carbons are traced, with all atoms shown for residues 113–118 (Tyr-Val-Tyr-Lys-Pro-Asn), in the upper left of the figure. The bound pdTp and Ca^{2+} (dotted sphere) of the nuclease complex are shown in green. The flexible loop around residue 50 is at the bottom of the figure. **(b)** Detailed view of the nucleotide binding pocket with the nuclease structure (red) superimposed on the backbone of the nuclease complex structure (blue) and the pdTp and Ca^{2+} (green). Tyr-113 and Tyr-115 which pack on the nucleotide base in the complex structure swing out of the binding pocket and pack against one another. Hydrogen bonds between the nucleotide phosphates and protein ligands (Lys-84, Tyr-85, Arg-87, Arg-35) are shown in amber. The side chains of the phosphate ligands are unchanged in the unliganded nuclease structure. **(c)** Detailed view of the Ca^{2+} binding region with the nuclease structure (red) superimposed on the backbone of the nuclease complex structure (blue) and the pdTp and Ca^{2+} (green). The water molecule which forms a bridged hydrogen bond between Glu-43 and the Ca^{2+} is represented by the blue sphere. The water molecule which occupies the Ca^{2+} site in the nuclease structure is represented by the red sphere.

Table X. Symmetry Related Hydrogen Bonds

Donor (D)			Acceptor (A)			D-A distance (Å)
Q	80	OE1	Q	106	NE2	2.98
R	81	N	E	135	OE2	2.88
T	82	OG1	E	135	OE1	2.82
K	70	NZ	D	19	OD1	2.78
K	70	NZ	E	43	OE2	2.71
K	70	NZ	D	21	OD2	2.96
T	13	OG1	Y	85	O	3.01
E	67	O	K	24	NZ	2.88
K	127	NZ	K	28	O	2.61
						Ave = 2.85

Nucleotide Phosphate Ligands

The final regions of interaction between the protein and bound ligands are the side chains of Arg-35, Lys-84, Tyr-85, and Arg-87 which position the 3′- and 5′-phosphates of pdTp in the nuclease complex. As shown in Figure 7b the side chains are unchanged in the absence of nucleotide. Mutual packing interactions between Lys-84 and Tyr-85 which hold the 3′-phosphate oxygens in the nuclease complex appear sufficient to correctly position the residues in the absence of nucleotide. Arg-35 and Arg-87 which form a pair of hydrogen bonds each with oxygen atoms of the 5′-phosphate remain fixed in the absence of the nucleotide, with two water molecules hydrogen bonded to Arg-87 in place of the phosphate oxygens. The side chain of Arg-35 is held in position by hydrogen bonds to the backbone oxygens of Leu-36 and Val-39. Arg-87 is anchored by a branched hydrogen bond to the side chain of Asp-83.

The high-resolution crystal structure of staphylococcal nuclease reported here provides a basis for the interpretation of mutational and physical data. A comparison of the structure with the high-resolution structure of the nuclease complex[2] with pdTp and Ca^{2+} indicates that the binding sites for the 3′- and 5′-phosphates preexist in the protein surface while the binding pocket for the base and the Ca^{2+} site are induced on binding.

ACKNOWLEDGMENTS

We thank Andy Howard for instruction on the Nicolet-Xentronics area detector system and XENGEN software, Axel Brünger for assistance with the XPLOR program package, and Pat Loll and Ed Lattman for providing us with the unpublished manuscript and coordinates of the nuclease complex structure. The coordinates will be submitted to the Brookhaven Protein Data Bank.

REFERENCES

1. Cotton, F. A., Hazen, E. E., Jr., Legg, M. J. Staphylococcal nuclease: Proposed mechanism of action based on structure of enzyme-thymidine 3′,5′-bisphosphate-calcium ion complex at 1.5 Å resolution. Proc. Natl. Acad. Sci. U.S.A. 76:2551–2555, 1979.
2. Loll, P. A., Lattman, E. E. The crystal structure of the ternary complex of staphylococcal nuclease, Ca^{2+}, and the inhibitor pdTp, refined at 1.65 Å. Proteins 5:183–201, 1989.
3. Cuatrecasas, P., Fuchs, S., Anfinsen, C. B. Catalytic properties and specificity of the extracellular nuclease of *Staphylococcus aureus*. J. Biol. Chem. 242;1541–1547, 1967.
4. Tucker, P. W., Hazen, E. E., Jr., Cotton, F. A. Staphylococcal nuclease reviewed: A prototypic study in contemporary enzymology. I. Isolation; physical and enzymatic properties. Mol. Cell. Biochem. 22:67–77, 1978.
5. Tucker, P. W., Hazen, E. E., Jr., Cotton, F. A. Staphylococcal nuclease reviewed: A prototypic study in contemporary enzymology. II. Solution studies of the nucleotide binding site and the effects of nucleotide binding. Mol. Cell. Biochem. 23:3–17, 1979.
6. Tucker, P. W., Hazen, E. E., Jr., Cotton, F. A. Staphylococcal nuclease reviewed: A prototypic study in contemporary enzymology. III. Correlation of the three-dimensional structure with the mechanisms of enzymatic action. Mol. Cell. Biochem. 23:67–86, 1979.
7. Tucker, P. W., Hazen, E. E., Jr., Cotton, F. A. Staphylococcal nuclease reviewed: A prototypic study in contemporary enzymology. IV. Nuclease as a model for protein folding. Mol. Cell. Biochem. 23:131–141, 1979.
8. Epstein, H. F., Schechter, A. N., Chen, R. F., Anfinsen, C. B. Folding of staphylococcal nuclease: Kinetic studies of two processes in acid renaturation. J. Mol. Biol. 60:499–508, 1971.
9. Calderon, R. O., Stolowich, N. J., Gerlt, J. A., Sturtevant, J. M. Thermal denaturation of staphylococcal nuclease. Biochemistry 24:6044–6049, 1985.
10. Shortle, D., Lin, B. Genetic analysis of staphylococcal nuclease: Identification of three intragenic "global" suppressors of nuclease-minus mutations. Genetics 110:539–555, 1985.
11. Shortle, D., Meeker, A. K. Mutant forms of staphylococcal nuclease with altered patterns of guanidine hydrochloride and urea denaturation. Proteins 1:81–89, 1986.
12. Serpersu, E. H., Shortle, D., Mildvan, A. S. Kinetic and magnetic resonance studies of effects of genetic substitution of a Ca^{2+}-liganding amino acid in staphylococcal nuclease. Biochemistry 25:68–77, 1986.
13. Sepersu, E. H., Shortle, D., Mildvan, A. S. Kinetic and magnetic resonance studies of active-site mutants of staphylococcal nuclease: Factors contributing to catalysis. Biochemistry 26:1289–1300, 1987.
14. Hynes, T. R., Kautz, R. A., Goodman, M. A., Gill, J. F., Fox, R. O. Transfer of a β-turn structure to a new protein context. Nature (London) 339:73–76, 1989.
15. Loll, P. J., Meeker, A. K., Shortle, D., Pease, M., Lattman, E. E. Crystallization and preliminary x-ray analysis of a quadruple mutant of staphylococcal nuclease. J. Biol. Chem. 263:18190–18192, 1988.
16. Evans, P. A., Kautz, R. A., Fox, R. O., Dobson, C. M. A magnetization-transfer nuclear magnetic resonance study of the folding of staphylococcal nuclease. Biochemistry 28: 362–370, 1989.
17. Alexandrescu, A. T., Mills, D. A., Ulrich, E. L., Chinami, M., Markley, J. L. NMR assignments of the four histidines of staphylococcal nuclease in native and denatured states. Biochemistry 27:2158–2165, 1988.
18. Torchia, D. A., Sparks, S. W., Bax, A. Staphylococcal nuclease: Sequential assignments on solution structure. Biochemistry 28:5509–5524, 1989.
19. Hendrickson, W. A. Stereochemically restrained refinement of macromolecular structures. Methods Enzymol. 115:252–270, 1985.
20. Stanislowski, A. G. Structural Studies of some molybdenum complexes of pyrazolylborate and of the enzyme, staphylococcal nuclease. Ph.D. thesis, Texas A&M University, 1976.
21. Bernstein, F. C., Koetzle, T. F., Williams, G. J. B., Meyer, E. F., Jr., Brice, M. D., Rodgers, J. R., Kennard, O., Shimanouchi, T., Tasumi, M. The Protein Data Bank: A computer-based archival file for macromolecular structures. J. Mol. Biol. 112:535–542, 1977.
22. Arnone, A., Bier, C. J., Cotton, F. A., Day, V. W., Hazen,

E.E., Richardson, D. C., Richardson, J. S. A high resolution structure of an inhibitor complex of the extracellular nuclease of *Staphylococcus aureus*. J. Biol. Chem. 245:2302–2316, 1971.
23. Arnone, A., Bier, C. J., Cotton, F. A., Hazen, E. E., Jr., Richardson, D. C., Richardson, J. S. The extracellular nuclease of *Staphylococcus aureus:* Structure of the native enzyme and an enzyme-inhibitor complex at 4 Å resolution. Proc. Natl. Acad. Sci. U.S.A. 64:420–427, 1969.
24. Howard, A. J., Gilliland, G. L., Finzel, B. C., Poulos, T. L., Ohlendorf, D. H., Salemme, F. R. The use of an imaging proportional counter in macromolecular crystallography. J. Appl. Crystallogr., 20:383–387, 1987.
25. Matthews, B. W., Czerwinski, E. W. Local scaling: A method to reduce systematic errors in isomorphous replacement and anomalous scattering measurements. Acta Crystallogr. A31:480–487, 1975.
26. Brünger, A. T., Kuriyan,J., Karplus, M. Crystallographic R factor refinement by molecular dynamics. Science 235: 458–460, 1987.
27. Brünger, A. T. Crystallographic refinement by simulated annealing: Application to a 2.8 Å resolution structure of aspartate aminotransferase. J. Mol. Biol. 203:803–816, 1988.
28. Jones, T. A. Interactive computer graphics: FRODO. Methods Enzymol. 115:252–270, 1985.
29. Luzatti, P. V. Traitement statistique des erreurs dans la determination des structures cristallines. Acta Crystallogr. 5:802–810, 1952.
30. Richardson, J. S. The anatomy and taxonomy of protein structure. Adv. Protein Chem. 34:167–339, 1981.
31. Sibanda, B. L., Thornton, J. M. β-Hairpin families in globular proteins. Nature (London) 316:170–174, 1985.
32. Marqusee, S., Baldwin, R. L. Helix stabilization by Glu^- . . . Lys^+ salt bridges in short peptides of *de novo* design. Proc. Natl. Acad. Sci. U.S.A. 84:8898–8902, 1987.
33. Evans, P. A., Dobson, C. M., Kautz, R. A., Hatfull, G., Fox, R. O. Proline isomerism in staphylococcal nuclease characterized by NMR and site-directed mutagenesis. Nature (London) 329:266–268, 1987.
34. Fox, R. O., Evans, P. A., Dobson, C. M. Multiple conformations of a protein demonstrated by magnetization transfer NMR spectroscopy. Nature (London) 320:192–194, 1986.
35. Lesk, A. M., Hardman, K. D. Computer-generated schematic diagrams of protein structures. Science 216:539–540, 1982.